ISTITUTO DI ANALISI DEI SISTEMI ED INFORMATICA
"Antonio Ruberti"
CONSIGLIO NAZIONALE DELLE RICERCHE

P. Palumbo, S. Panunzi, A. De Gaetano

QUALITATIVE BEHAVIOR OF A FAMILY OF DELAY-DIFFERENTIAL MODELS OF THE GLUCOSE-INSULIN SYSTEM

R. 620 Novembre 2004

Pasquale Palumbo – CNR, Istituto di Analisi dei Sistemi ed Informatica "A. Ruberti", Viale Manzoni 30, 00185 Roma, Italy. Email: palumbo@iasi.cnr.it.

Simona Panunzi – CNR, Istituto di Analisi dei Sistemi ed Informatica "A. Ruberti", BioMatLab, Università Cattolica del Sacro Cuore, Largo A. Gemelli 8, 00168 Roma, Italy. Email: simona.panunzi@biomatematica.it.

Andrea De Gaetano – CNR, Istituto di Analisi dei Sistemi ed Informatica "A. Ruberti", BioMatLab, Università Cattolica del Sacro Cuore, Largo A. Gemelli 8, 00168 Roma, Italy. Email: andrea.degaetano@biomatematica.it.

ISSN: 1128–3378

Collana dei Rapporti
dell'Istituto di Analisi dei Sistemi ed Informatica, CNR

viale Manzoni 30, 00185 ROMA, Italy

tel. ++39-06-77161
fax ++39-06-7716461
email: iasi@iasi.rm.cnr.it
URL: http://www.iasi.rm.cnr.it

Abstract

A family of delay-differential models of the glucose-insulin system is introduced, whose members represent adequately the Intra-Venous Glucose Tolerance Test and allied experimental procedures of diabetological interest. All the models in the family admit positive bounded unique solutions for any positive initial condition and are persistent. The models agree with the physics underlying the experiments, and they all present a unique positive equilibrium point.

Local stability is investigated in a pair of interesting member models: one, a discrete-delays differential system; the other, a distributed-delay system reducing to an ordinary differential system evolving on a suitably defined extended state space. In both cases conditions are given on the physical parameters in order to ensure the local asymptotic stability of the equilibrium point. These conditions are always satisfied, given the actual parameter estimates obtained experimentally. A study of the global stability properties is performed, but while from simulations it could be conjectured that the models considered are globally asymptotically stable, sufficient stability criteria, formally derived, are not actually satisfied for physiological parameters values. Given the practical importance of the models studied, further analytical work may be of interest to conclusively characterize their behavior.

Key words: Delay-Differential Systems, Integro-Differential Systems, Glucose-Insulin Homeostasis, Stability analysis.

1. Introduction

The modeling of the glucose-insulin system is an appealing and challenging topic in biomathematics and many different models have been presented in the last decades, mostly referred to the experimental framework of the *Intra Venous Glucose Tolerance Test* (IVGTT), where a bolus of glucose is administered intra-venously and glucose and insulin concentrations are frequently sampled (see e.g. the ODEs of the Minimal Model [1, 17], or the more recent integro-differential equations models of [2, 11, 13]). An interesting survey on a very wide class of most significant models available in the literature and the software tools related to them can be found in [12]. The interest in modelling this physiological system stems in part from its relative simplicity, in part from the social impact of its derangement (giving rise to the widespread disease Diabetes Mellitus), in part from the actual need of the diabetologists for a method capable of delivering a single numerical index, diagnostic of the insulin sensitivity of the patient.

The fact that several attempts at modeling the glucose-insulin system have been made in the past points to the actual difficulty in constructing a model which is at the same time mathematically coherent, statistically robust and physiologically meaningful. In other words, the model should exhibit satisfactory properties of the solutions, its parameters should be statistically estimable with sufficient precision from data sets obtained from standard experimental procedures, and it should conform to established physiological concepts. So far, indeed, no single model exhibiting simultaneously all of these features has been proposed.

In this paper a family of delay-differential models of the glucose-insulin system is investigated with respect to the behavior of the resulting solutions. The family considered is similar to that studied by Li et al. [8] with respect to which it introduces the possibility of generally considering delays both in the insulin action on tissue glucose uptake and in the glucose action on pancreatic insulin secretion. According to the family of models presented, the glucose-insulin dynamics is characterized by coupled integro-differential equations: by choosing the kernels of the convolution integrals among a set of admissible functions, different models can be obtained. Two meaningful choices for the kernels give rise to discrete-delay differential equations or to ordinary differential equations on a suitably defined extended state space. From a physiological point of view, these models incorporate an explicit delay in the control action exerted by glucose on pancreatic insulin secretion; express the effect of (delayed) glucose by a saturable sigmoidal function; and include second-order control of net glucose uptake by circulating insulin. One model of the family has been identified from IVGTT data [14], providing excellent results in terms of parameter estimation. Since these models appear statistically and physiologically promising, the purpose of this work is, then, that of studying their mathematical properties with some degree of generality.

The family of delay-differential systems is presented in detail in the next section. In Section three it is proven that each of these models admits positive bounded unique solutions for any positive initial condition and is persistent. Section four deals with the stability properties of the models: all the models in the considered family have a unique positive equilibrium point. For both specific models previously mentioned, conditions are given on the physical parameters in order to ensure the local asymptotic stability of the equilibrium point. According to the estimates [14] and to the physics underlying the parameter values, these conditions are always satisfied. Sufficient conditions are also given to ensure the global attractivity of the equilibrium point for a generic model of the family, which however are not satisfied for the two specific models, given the corresponding parameter estimates experimentally obtained. In Section five simulation results are reported, dealing with the two specific models, for meaningful sets of

parameters: they conform to the theoretical results and showcase the conditions under which limit cycles may occur. The parameter identification procedure is briefly described in Section six.

2. Models considered

Denote $G(t)$, [mM], $I(t)$, [pM], plasma glycemia and insulinemia, respectively; the proposed class of dynamical models of the glucose-insulin homeostasis is written according to the following generic delay-differential system:

$$\left\{\begin{array}{l} \dfrac{dG}{dt} = -K_{xg}G(t) - K_{xgi}G(t)\widetilde{I}(t) + \dfrac{T_{gh}}{V_G}, \\ \dfrac{dI}{dt} = -K_{xi}I(t) + \dfrac{T_{iGmax}}{V_I} f\big(\widetilde{G}(t)\big), \end{array}\right. \qquad f\big(\widetilde{G}(t)\big) = \frac{\left(\frac{\widetilde{G}(t)}{G^*}\right)^{\gamma}}{1+\left(\frac{\widetilde{G}(t)}{G^*}\right)^{\gamma}}. \tag{2.1}$$

where:
- K_{xg}, [min^{-1}], is the rate of insulin-independent glucose uptake;
- K_{xgi}, [min^{-1} pM^{-1}], is the rate of glucose uptake by tissues (insulin-dependent) per pM of plasma insulin concentration;
- T_{gh}, [min^{-1}(mmol/kgBW)], is the net balance between hepatic glucose output and insulin-independent zero-order glucose tissue uptake (mainly by the brain, supposed constant throughout the experiment);
- V_G, [L/kgBW], is the apparent distribution volume for glucose;
- K_{xi}, [min^{-1}], is the apparent first-order disappearance rate constant for insulin;
- T_{iGmax}, [min^{-1}(pmol/kgBW)], is the maximal rate of second-phase insulin release;
- V_I, [L/kgBW], is the apparent distribution volume for insulin;
- γ, [♯], is the progressivity with which the pancreas reacts to circulating glucose concentrations. If γ were zero, the pancreas would not react to circulating glucose at all; if γ were 1, the pancreas would respond according to a Michaelis-Menten dynamics, where $G^\star$ is the glucose concentration of half-maximal insulin secretion; when γ is greater than 1 (as is usually the case), the pancreas responds according to a sigmoidal function.
- G^* [mM] is the glycemia at which the insulin release is the half of its maximal rate; at a glycemia equal to G^* corresponds an insulin secretion equal to $T_{iGmax}/2$.
- $\widetilde{G}(t)$ and $\widetilde{I}(t)$ are the following time-integrals of the glucose and insulin concentrations:

$$\widetilde{G}(t) = \int_0^{\tau_g} \omega_g(\theta)G(t-\theta)d\theta, \qquad \widetilde{I}(t) = \int_0^{\tau_i} \omega_i(\theta)I(t-\theta)d\theta, \tag{2.2}$$

where the kernels $\omega_g : [0,\tau_g] \mapsto I\!R^+$, $\omega_i : [0,\tau_i] \mapsto I\!R^+$ are non-negative, square integrable functions, such that:

$$\int_0^{\tau_g} \omega_g(\theta)d\theta = 1, \qquad \int_0^{\tau_i} \omega_i(\theta)d\theta = 1, \tag{2.3}$$

and:

$$\exists\ T_g, T_i : \qquad \int_0^{\tau_g} \theta\omega_g(\theta)d\theta \leq T_g < +\infty, \qquad \int_0^{\tau_i} \theta\omega_i(\theta)d\theta \leq T_i < +\infty, \tag{2.4}$$

From (2.1), it is apparent that:

- the insulin-independent glucose uptake, $-K_{xg}G(t)$, is a linear function of the plasma glycemia;
- the insulin-dependent glucose uptake, $-K_{xgi}G(t)\widetilde{I}(t)$, is a bilinear function of the pair $\big(G(t), \widetilde{I}(t)\big)$;
- the net glucose production, T_{gh}/V_G, is a constant term: during a standard IVGTT no exogenous glucose infusions are administered;
- insulin degradation, $-K_{xi}I(t)$, is a linear function of the plasma insulinemia;

The Jacobian of f is reported below for ease of reference:

$$\frac{df}{dG} = \frac{\gamma}{G^*} \frac{\left(\frac{G}{G^*}\right)^{\gamma-1}}{\left(1 + \left(\frac{G}{G^*}\right)^{\gamma}\right)^2}. \tag{2.5}$$

Remark 2.1. In the following Sections the existence of a unique equilibrium point, reflecting the basal levels of glycemia and insulinemia, G_b, [mM], and I_b, [pM], respectively, will be proved. Both basal levels are measured, so that a pair of model parameters need not be estimated, but are readily computed according to the equilibrium equations:

$$T_{gh} = V_G G_b (K_{xg} + K_{xgi} I_b), \qquad T_{iGmax} = \frac{V_I K_{xi} I_b}{f(G_b)}. \tag{2.6}$$

Remark 2.2. All model parameters previously defined are strictly positive, except for K_{xg}, which may also be zero. Such a case, in fact, has a very plausible physiological motivation because the insulin-independent glucose uptake may be completely modeled by the constant net balance term T_{gh}. Experimental results support this interpretation in many subjects [14].

Remark 2.3. Model (2.1) reduces to an element of the class of the glucose-insulin models defined in [11] in case of $\widetilde{I}(t) \equiv I(t)$ (i.e. $\omega_i(\theta) = \delta(\theta)$) and K_{xg} strictly positive.

3. General analysis of the solutions

In this section we prove that the delay-differential model (2.1) admits a unique positive bounded solution for any positive initial condition and that, moreover, the model is persistent. According to widely adopted notation [6, 8], let $\tau = \max\{\tau_g, \tau_i\}$ and denote with $\mathcal{C}_\tau = C\big([-\tau, 0], I\!R^2\big)$ the Banach space of all the continuous functions mapping $[-\tau, 0]$ into $I\!R^2$, with the topology of uniform convergence. Then, model (2.1) consists of an RFDE (*Retarded Functional Differential Equation*) on $\mathcal{C}_\tau$; by defining $X(t) = \big(G(t) \;\; I(t)\big)^T \in I\!R^2$, it may be written in the following more compact form:

$$\frac{dX}{dt} = F(X_t) \quad \text{with} \quad F : \mathcal{C}_\tau \mapsto I\!R^2, \quad \text{and} \quad X_t(\theta) = X(t+\theta), \quad \theta \in [-\tau, 0]. \tag{3.1}$$

According to the existence and uniqueness conditions for RFDEs (see [6, 8] and references therein), if the initial condition $X_0 = \phi$ belongs to $\mathcal{C}_\tau$, there is a unique solution of system (3.1) through ϕ, because $F(\cdot)$ is continuous and Lipschitz in each compact set of $\mathcal{C}_\tau$. Moreover, solutions are continuous w.r.t. to both the initial condition $\phi \in \mathcal{C}_\tau$ and the model parameters. Absolutely continuous solutions are also ensured in the case of suitable discontinuous initial conditions, for instance for initial conditions ϕ uniformly continuous on $[-\tau, 0)$, but with $\phi(0^-) \neq \phi(0)$, see [7, pg.101]. The need for establishing existence in this case arises because the IVGTT protocol calls for an impulsive increase of glycemia at time zero, making the initial condition (theoretically) discontinuous. In this case, the initial conditions for (2.1) are determined by the intra-venous instantaneous injection of a glucose bolus D_g, [mmol/kgBW], so that:

$$\begin{aligned} &G(t) \equiv G_b, \qquad t \in [-\tau_g, 0), \qquad && I(t) \equiv I_b, \qquad t \in [-\tau_i, 0), \\ &G(0) = G_b + G_\Delta, && I(0) = I_b + I_\Delta G_\Delta, \end{aligned} \tag{3.2}$$

with:

- $G_\Delta = D_g/V_G$, [mM], the theoretical increase in plasma glucose concentration over basal glucose concentration at time zero after the instantaneous administration and redistribution of the I.V. glucose bolus D_g;
- I_Δ, [pM/mM], the first-phase insulin concentration increase per mM increase in glucose concentration at time zero due to the injected bolus.

The following theorems investigate positiveness, boundedness and persistency of the models.

Theorem 3.1. *System* (2.1) *admits positive solutions for any positive initial condition.*

Proof. Let $G(0) > 0$. According to the continuity of the solution of a differential equation, $G(t)$ would become non-positive if there existed a $t_0 > 0$ such that $G(t_0) = 0$ and $G(t) > 0$ for any $0 \leq t < t_0$. Then, necessarily, $\frac{dG}{dt}\big|_{t=t_0} \leq 0$, which is a contradiction because:

$$\left.\frac{dG}{dt}\right|_{t=t_0} = -K_{xg}G(t_0) - K_{xgi}G(t_0)\widetilde{I}(t_0) + \frac{T_{gh}}{V_G} = \frac{T_{gh}}{V_G} > 0. \tag{3.3}$$

This proves that, if $G(0) > 0$, $G(t)$ never vanishes and is always positive. Similarly it can be proven that, if $I(0) > 0$, also $I(t)$ never vanishes and is always positive: let $I(0) > 0$ and assume that $\exists\ t_0 > 0$ such that $I(t_0) = 0$ and $I(t) > 0$ for any $0 \leq t < t_0$. Then, necessarily, $\frac{dI}{dt}\big|_{t=t_0} \leq 0$, which is a contradiction because:

$$\left.\frac{dI}{dt}\right|_{t=t_0} = -K_{xi}I(t_0) + f\big(\widetilde{G}(t_0)\big) = f\big(\widetilde{G}(t_0)\big) > 0. \tag{3.4}$$

∎

Theorem 3.2. *System* (2.1) *is a persistent model.*

Proof. According to Remark 2.2, the proof is valid for $K_{xg} \geq 0$ (i.e. K_{xg} may well be zero throughout). Recall that a model is persistent if there exists a pair of positive real numbers (m, M) such that:

$$\exists\, \bar{t}: \quad 0 < m < X_i(t) < M < +\infty, \quad \forall t \geq \bar{t}, \tag{3.5}$$

for each component X_i of the state vector. Denote:

$$G_m = \liminf_{t \mapsto +\infty} G(t), \qquad G_M = \limsup_{t \mapsto +\infty} G(t), \qquad I_m = \liminf_{t \mapsto +\infty} I(t), \qquad I_M = \limsup_{t \mapsto +\infty} I(t). \tag{3.6}$$

The proof is achieved by proving the following four statements:

$$1)\ I_M < +\infty, \qquad 2)\ G_m > 0, \qquad 3)\ I_m < 0, \qquad 4)\ G_M < +\infty.$$

Step 1. In order to show the boundedness of the evolution of insulin, assume that $I_M = +\infty$, which means, due to continuity:

$$\exists \{t_n\} \subset [0, +\infty): \quad \lim_{n \mapsto \infty} t_n = +\infty, \quad \lim_{n \mapsto \infty} I(t_n) = +\infty, \quad \text{with} \quad \left.\frac{dI}{dt}\right|_{t=t_n} \geq 0. \tag{3.7}$$

But:

$$\left.\frac{dI}{dt}\right|_{t=t_n} = -K_{xi} I(t_n) + f\big(\widetilde{G}(t_n)\big) \mapsto -\infty, \tag{3.8}$$

which is a contradiction, so that $I_M < +\infty$.

Step 2. Suppose $G_m < +\infty$ (otherwise $G_m > 0$ is trivially verified). Due to continuity:

$$\exists \{t_n\} \subset [0, +\infty): \quad \lim_{n \mapsto \infty} t_n = +\infty, \quad \lim_{n \mapsto \infty} G(t_n) = G_m, \quad \text{with} \quad \lim_{n \mapsto \infty} \left.\frac{dG}{dt}\right|_{t=t_n} = 0, \tag{3.9}$$

that means:

$$\begin{aligned} 0 = \lim_{n \mapsto \infty} \left(-K_{xg} G(t_n) - K_{xgi} G(t_n) \widetilde{I}(t_n) + \frac{T_{gh}}{V_G} \right) &\geq -K_{xg} G_m - K_{xgi} G_m I_M + \frac{T_{gh}}{V_G} \\ \implies \quad \frac{T_{gh}}{V_G} &\leq K_{xg} G_m + K_{xgi} G_m I_M. \end{aligned} \tag{3.10}$$

According to the inequality (3.10), it is $G_m > 0$, otherwise it would be $T_{gh}/V_G \leq 0$.

Step 3. From Step 1, it follows that $I_m \leq I_M < +\infty$. Due to continuity:

$$\exists \{t_n\} \subset [0, +\infty): \quad \lim_{n \mapsto \infty} t_n = +\infty, \quad \lim_{n \mapsto \infty} I(t_n) = I_m, \quad \text{with} \quad \lim_{n \mapsto \infty} \left.\frac{dI}{dt}\right|_{t=t_n} = 0, \tag{3.11}$$

that means:

$$\begin{aligned} 0 = \lim_{n \mapsto \infty} \left(-K_{xi} I(t_n) + \frac{T_{iGmax}}{V_I} f\big(\widetilde{G}(t_n)\big) \right) &\geq -K_{xi} I_m + \frac{T_{iGmax}}{V_I} f\big(G_m\big) \\ \implies \quad \frac{T_{iGmax}}{V_I} f\big(G_m\big) &\leq K_{xi} I_m. \end{aligned} \tag{3.12}$$

According to inequality (3.12), it follows that $I_m > 0$, otherwise it would be $T_{iGmax}/V_I < 0$.

Step 4. In order to show the boundedness of the evolution of glucose, assume that $G_M = +\infty$, which means, due to continuity:

$$\exists\{t_n\} \subset [0, +\infty) : \quad \lim_{n\mapsto\infty} t_n = +\infty, \quad \lim_{n\mapsto\infty} G(t_n) = +\infty, \quad \text{with} \quad \left.\frac{dG}{dt}\right|_{t=t_n} \geq 0. \tag{3.13}$$

But:

$$\left.\frac{dG}{dt}\right|_{t=t_n} = -K_{xg}G(t_n) - K_{xgi}G(t_n)\widetilde{I}(t_n) + \frac{T_{gh}}{V_G} \mapsto -\infty, \tag{3.14}$$

which is a contradiction, so that $G_M < +\infty$.

∎

Remark 3.3. As a consequence of Theorems 3.1 and 3.2, system (2.1) admits positive bounded solutions for any positive initial condition.

Remark 3.4. It is easy to verify at this point that the following inequalities hold:

$$\frac{T_{iGmax}}{V_I} f(G_m) \leq K_{xi} I_m \leq K_{xi} I_M \leq \frac{T_{iGmax}}{V_I} f(G_M), \tag{3.15a}$$

$$K_{xg}G_M + K_{xgi}G_M I_m \leq \frac{T_{gh}}{V_G} \leq K_{xg}G_m + K_{xgi}G_m I_M. \tag{3.15b}$$

4. Equilibria and stability analysis

It is shown here that each of the models (2.1) admits a unique positive equilibrium point. Conditions are given to ensure global attractivity; local asymptotic stability is proven for a pair of significative models.

Theorem 4.1. *System* (2.1) *has a unique positive equilibrium point, which consists of the basal glucose and insulin concentrations,* G_b, I_b.

Proof. Each equilibrium point (G_e, I_e) has to satisfy the following equations:

$$\begin{cases} K_{xg}G_e + K_{xgi}G_e I_e = \dfrac{T_{gh}}{V_G} \\ K_{xi} I_e = \dfrac{T_{iGmax}}{V_I} f(G_e) \end{cases} \quad \Longrightarrow \quad \varphi(G_e) = \frac{T_{gh}}{V_G} - K_{xg}G_e - \frac{K_{xgi}T_{iGmax}G_e f(G_e)}{K_{xi}V_I} = 0. \tag{4.1}$$

Note that $\varphi(0) = T_{gh}/V_G > 0$ and:

$$\frac{d\varphi}{dG} = -K_{xg} - \frac{K_{xgi}T_{iGmax}f(G)}{K_{xi}V_I} - \frac{K_{xgi}T_{iGmax}Gf'(G)}{K_{xi}V_I} < 0, \qquad \forall G \geq 0, \tag{4.2}$$

in that $f(\cdot)$, $f'(\cdot)$ are both positive for positive entries. Then $\varphi(\cdot)$ is a decreasing function for positive argument, starting from a positive value at zero, and it may hence have at most one positive root. The existence of such a root is ensured by the limit:

$$\lim_{G\mapsto+\infty} \varphi(G) = \lim_{G\mapsto+\infty} -G\left(K_{xg} + \frac{K_{xgi}T_{iGmax}f(G)}{K_{xi}V_I}\right) + \frac{T_{gh}}{V_G} = -\infty. \tag{4.3}$$

∎

Remark 4.2. It has to be stressed that, in order to check the global attractiveness of the equilibrium point, the sufficient conditions proposed in [11] (Thm.3.1, Thm.3.2, Thm.3.3 and corollaries) are not fulfilled for the present family of models, even assuming $K_{xg} > 0$ and $\widetilde{I}(t) = I(t)$. Such a situation occurs for any set of parameters, because it depends structurally on the mathematical formulation of the functions chosen to describe insulin-dependent glucose uptake and pancreatic insulin secretion. It is worthwhile, then, to endeavor to find some different criterion to ensure global stability of the equilibrium point.

The following Lemmas show that under suitably defined conditions on the parameters, the unique equilibrium point is globally attractive. The idea is based on the ω-limit set for a given initial condition ϕ, associated to an RFDE of the type (3.1). Such an approach has been followed in [2] in a similar framework, and can be generalized for scalar delay-differential equations [10]. The ω-limit set is defined as the set of all limit points of the set $\{X_t,\ t \geq 0\}$ [6].

As a preliminary step, recall that for any scalar differential inequality of the type:

$$\frac{dX}{dt} \leq -\alpha X(t) + \beta, \qquad \alpha, \beta > 0, \tag{4.4}$$

it is:

$$X(t) \leq e^{-\alpha t} X(0) + \frac{\beta}{\alpha}\big(1 - e^{-\alpha t}\big). \tag{4.5}$$

Moreover:

$$X(0) \leq \frac{\beta}{\alpha} \qquad \Longrightarrow \qquad X(t) \leq \frac{\beta}{\alpha}, \qquad \forall t \geq 0. \tag{4.6}$$

Similarly, by changing the inequality in (4.4):

$$\frac{dX}{dt} \geq -\alpha X(t) + \beta \qquad \Longrightarrow \qquad X(t) \geq e^{-\alpha t} X(0) + \frac{\beta}{\alpha}\big(1 - e^{-\alpha t}\big), \tag{4.7}$$

with:

$$X(0) \geq \frac{\beta}{\alpha} \qquad \Longrightarrow \qquad X(t) \geq \frac{\beta}{\alpha}, \qquad \forall t \geq 0. \tag{4.8}$$

Definition 4.3. Consider a solution $S = (G, I)$ of system (2.1) for a generic initial condition ϕ. Let $\Xi = (\xi_G, \xi_I) \in \mathcal{C}_\tau$ be a point in the nonempty ω-limit set of ϕ (see e.g. [2], [10]). We define $\bar{S} = (\bar{G}, \bar{I})$ the solution of (2.1) with initial condition Ξ.

Notice that, according to the positive invariance of the ω-limit set [16], the solution $\bar{S}_t$ belongs itself to the ω-limit set of ϕ, and can be extended as a solution for negative real t so that $\bar{S}_t$ is in the ω-limit set for every t. In the following G_M, G_m, I_M, I_m are defined as in (3.6) and are referred to the solution S in Definition 4.3.

Lemma 4.4. *The evolution $\bar{G}(t)$ is bounded by the following sequences of upper and lower bounds:*

$$m_k \leq \bar{G}(t) \leq M_k, \qquad m_k = h(M_k), \qquad M_{k+1} = h(m_k), \tag{4.9}$$

with:

$$M_0 = \frac{G_b(K_{xg} + K_{xgi} I_b)}{K_{xg}}, \qquad \textit{and} \qquad h(x) = \frac{G_b(K_{xg} + K_{xgi} I_b)}{K_{xg} + \frac{K_{xgi} I_b f(x)}{f(G_b)}}. \tag{4.10}$$

Proof. The Lemma is proved by induction. Assume there exists M_k such that $\bar{G}(t) \leq M_k$. Then, the insulin time derivative is majored as follows:

$$\frac{d\bar{I}}{dt} \leq -K_{xi}\bar{I}(t) + \frac{T_{iGmax}}{V_I} f(M_k), \tag{4.11}$$

therefore, for any arbitrary $t_0 \leq t$:

$$\bar{I}(t) \leq e^{-K_{xi}(t-t_0)}\bar{I}(t_0) + \frac{T_{iGmax} f(M_k)}{V_I K_{xi}}\big(1 - e^{-K_{xi}(t-t_0)}\big). \tag{4.12}$$

Recall that $\bar{I}(t)$ is a bounded evolution so that, taking $t_0 \mapsto -\infty$, it follows that:

$$\bar{I}(t) \leq \frac{T_{iGmax} f(M_k)}{V_I K_{xi}}. \tag{4.13}$$

According to (4.13), the glucose time derivative is minored as follows:

$$\frac{d\bar{G}}{dt} \geq -\left(K_{xg} + K_{xgi}\frac{T_{iGmax} f(M_k)}{V_I K_{xi}}\right)\bar{G}(t) + \frac{T_{gh}}{V_G}, \tag{4.14}$$

therefore, for any arbitrary $t_0 \leq t$:

$$\begin{aligned}\bar{G}(t) \geq\ & e^{-\left(K_{xg} + K_{xgi}\frac{T_{iGmax} f(M_k)}{V_I K_{xi}}\right)(t-t_0)}\bar{G}(t_0) \\ & + \frac{T_{gh}}{V_G\left(K_{xg} + K_{xgi}\frac{T_{iGmax} f(M_k)}{V_I K_{xi}}\right)}\left(1 - e^{-\left(K_{xg} + K_{xgi}\frac{T_{iGmax} f(M_k)}{V_I K_{xi}}\right)(t-t_0)}\right).\end{aligned} \tag{4.15}$$

Recall that $\bar{G}(t)$ is a bounded evolution so that, taking $t_0 \mapsto -\infty$, it follows that:

$$\bar{G}(t) \geq m_k = h(M_k), \qquad \text{with} \qquad h(x) = \frac{T_{gh}}{V_G\left(K_{xg} + K_{xgi}\frac{T_{iGmax} f(x)}{V_I K_{xi}}\right)}. \tag{4.16}$$

Taking into account the relationships among T_{gh}, T_{iGmax} and the basal values G_b, I_b (2.6), it readily appears that the function $h(\cdot)$ is the same as that defined in (4.10). According to (4.16), the insulin time derivative is minored as follows:

$$\frac{d\bar{I}}{dt} \geq -K_{xi}\bar{I}(t) + \frac{T_{iGmax}}{V_I} f(m_k), \tag{4.17}$$

therefore, for any arbitrary $t_0 \leq t$:

$$\bar{I}(t) \geq e^{-K_{xi}(t-t_0)}\bar{I}(t_0) + \frac{T_{iGmax} f(m_k)}{V_I K_{xi}}\big(1 - e^{-K_{xi}(t-t_0)}\big), \tag{4.18}$$

from which, taking $t_0 \mapsto -\infty$, it follows that:

$$\bar{I}(t) \geq \frac{T_{iGmax} f(m_k)}{V_I K_{xi}}. \tag{4.19}$$

Finally, according to (4.19), the glucose time derivative is majored as follows:

$$\frac{d\bar{G}}{dt} \leq -\left(K_{xg} + K_{xgi}\frac{T_{iGmax}f(m_k)}{V_I K_{xi}}\right)\bar{G}(t) + \frac{T_{gh}}{V_G}, \tag{4.20}$$

therefore, for any arbitrary $t_0 \leq t$:

$$\begin{aligned}\bar{G}(t) \leq\ & e^{-\left(K_{xg}+K_{xgi}\frac{T_{iGmax}f(m_k)}{V_I K_{xi}}\right)(t-t_0)}\bar{G}(t_0) \\ & + \frac{T_{gh}}{V_G\left(K_{xg} + K_{xgi}\frac{T_{iGmax}f(m_k)}{V_I K_{xi}}\right)}\left(1 - e^{-\left(K_{xg}+K_{xgi}\frac{T_{iGmax}f(m_k)}{V_I K_{xi}}\right)(t-t_0)}\right),\end{aligned} \tag{4.21}$$

from which, taking $t_0 \mapsto -\infty$, it follows that:

$$\bar{G}(t) \leq M_{k+1} = \frac{T_{gh}}{V_G\left(K_{xg} + K_{xgi}\frac{T_{iGmax}f(m_k)}{V_I K_{xi}}\right)} = h(m_k). \tag{4.22}$$

The initial step for M_0 is readily obtained by majoring the glucose time derivative as follows:

$$\frac{d\bar{G}}{dt} \leq -K_{xg}\bar{G}(t) + \frac{T_{gh}}{V_G}, \tag{4.23}$$

therefore, for any arbitrary $t_0 \leq t$:

$$\bar{G}(t) \leq e^{-K_{xg}(t-t_0)}\bar{G}(t_0) + \frac{T_{gh}}{V_G K_{xg}}\big(1 - e^{-K_{xg}(t-t_0)}\big), \tag{4.24}$$

from which, taking $t_0 \mapsto -\infty$, we have that:

$$\bar{G}(t) \leq \frac{T_{gh}}{V_G K_{xg}} = \frac{G_b(K_{xg} + K_{xgi}I_b)}{K_{xg}} = M_0. \tag{4.25}$$

∎

Lemma 4.5. *Consider the sequences of bounds* $\{M_k\}$, $\{m_k\}$ *in Lemma* 4.4. *Then:*
i) $\{M_k\}$ *is a bounded monotone decreasing sequence;*
ii) $\{m_k\}$ *is a bounded monotone increasing sequence.*

Proof. From (4.9) we can write:

$$M_{k+1} = h\big(h(M_k)\big), \qquad m_{k+1} = h\big(h(m_k)\big). \tag{4.26}$$

Note that the function $h(x)$ is monotonically decreasing in x, so that $h\big(h(x)\big)$ is monotonically increasing in x. It means that, if $M_k \leq M_{k-1}$, then:

$$M_{k+1} = h\big(h(M_k)\big) \leq h\big(h(M_{k-1})\big) = M_k, \qquad m_k = h(M_k) \geq h(M_{k-1}) = m_{k-1}. \tag{4.27}$$

As far as the initial step of the induction is concerned, taking into account the computation of M_0 in (4.10):

$$M_1 = h(m_0) = \frac{G_b(K_{xg} + K_{xgi}I_b)}{K_{xg} + \frac{K_{xgi}I_b f(m_0)}{f(G_b)}} \leq \frac{G_b(K_{xg} + K_{xgi}I_b)}{K_{xg}} = M_0. \tag{4.28}$$

∎

Theorem 4.6. *Assume the following condition holds true among the model parameters:*

$$\frac{K_{xgi} I_b \gamma}{1 + \left(\frac{G_b}{G^*}\right)^{\gamma}} \leq K_{xg} + K_{xgi} I_b. \tag{4.29}$$

Then, the equilibrium point is globally attractive.

Proof. Consider the evolution $\bar{S}$ given by Definition 4.3. According to Lemmas 4.4 and 4.5, the glucose evolution is bounded by monotone increasing/decreasing sequences:

$$m_0 \leq m_1 \leq \ldots \leq m_k \leq \ldots \leq \bar{G}(t) \leq \ldots \leq M_k \leq \ldots \leq M_1 \leq M_0, \tag{4.30}$$

with $M_{k+1} = h\big(h(M_k)\big)$ and $m_{k+1} = h\big(h(m_k)\big)$. By consequence, both the sequences are converging. If the function $h\big(h(\cdot)\big)$ admits a unique fixed point, both the sequences converge to the same limit, so forcing the evolution of $\bar{G}(t)$ to be constant and equal to this limit. As a matter of fact, $\bar{I}(t)$ is also forced to be constant, for instance from inequality (3.15a). On the other hand, by definition, $\bar{S}$ has the initial condition in the ω-limit set of a generic solution of (2.1), that means the ω-limit set of any generic solution consists of the only fixed point of $h\big(h(\cdot)\big)$, and such a point results to be necessarily the equilibrium point of the system.

In order to find the fixed points of $h\big(h(\cdot)\big)$, consider the equation:

$$\Gamma(x) = x - h\big(h(x)\big) = 0. \tag{4.31}$$

It is easy to verify that:

$$\Gamma(0) = -h\big(h(0)\big) < 0 \qquad \text{and} \qquad \lim_{x \mapsto +\infty} \Gamma(x) = +\infty, \tag{4.32}$$

so that, by continuity, there exist at least one solution of (4.31). Compute the Jacobian of $\Gamma(x)$:

$$\frac{d\Gamma}{dx} = 1 - \left.\frac{dh}{dz}\right|_{z=h(x)} \cdot \frac{dh}{dx} \qquad \text{with} \qquad \frac{dh}{dx} = -\frac{G_b I_b K_{xgi}(K_{xg} + K_{xgi} I_b)}{f(G_b)\left(K_{xg} + \frac{K_{xgi} I_b f(x)}{f(G_b)}\right)^2} \cdot \frac{df}{dx}, \tag{4.33}$$

and df/dx as in (2.5). After some computations, it can be seen that:

i) if condition (4.29) holds as an equality, the Jacobian of $\Gamma(x)$ vanishes only in $x = G_b$ and is always non-negative: $x = G_b$ is the only root of $\Gamma(x) = 0$;

ii) if condition (4.29) holds true as a strict inequality, the Jacobian never vanishes and is always positive, so ensuring that $x = G_b$ is the only root of $\Gamma(x) = 0$;

iii) if condition (4.29) is not true, $x = G_b$ is one of three roots of $\Gamma(x) = 0$.

Only conditions i) and ii) ensure global attractiveness for the equilibrium point.

∎

Remark 4.7. This result is, however, of limited usefulness in the present case (as it also happens with other theoretical conditions on the model parameters, *sufficient* for global stability of the model). In fact, when inserting into (4.29) parameter values making physiological sense, such as are given from statistical estimation on real patients' data, the condition is not verified.

For instance, there are statistical and physiological reasons for which parameter K_{xg} may be zero. In this case, condition (4.29) becomes:

$$\frac{\gamma}{1+\left(\frac{G_b}{G^*}\right)^{\gamma}} \leq 1, \tag{4.34}$$

which is trivially verified for $\gamma \leq 1$. However, $\gamma \leq 1$ rarely happens in normal subjects and the result is that condition (4.34) is fulfilled in only about 3% of the normal subjects examined. On the other hand, in the sequel, *necessary* and *sufficient* conditions will be given for the local stability, which are easily verified on a wide range of realistic parameter values.

Global attractiveness and local stability determine global asymptotic stability of the equilibrium point. Local stability strongly depends on the choice of the kernels ω_g, ω_i in (2.2). If both the kernels are impulsive functions:

$$\omega_g(t) = \delta(t-\tau_g), \qquad \omega_i(t) = \delta(t-\tau_i), \tag{4.35}$$

the following discrete-delays differential equations system is obtained:

$$\begin{cases} \dfrac{dG}{dt} = -K_{xg}G(t) - K_{xgi}G(t)I(t-\tau_i) + \dfrac{T_{gh}}{V_G}, \\ \dfrac{dI}{dt} = -K_{xi}I(t) + \dfrac{T_{iGmax}}{V_I} f\big(G(t-\tau_g)\big); \end{cases} \tag{4.36}$$

where τ_g is the apparent delay with which the pancreas varies secondary insulin release in response to varying plasma glucose concentrations, and τ_i is the delay with which insulin acts in stimulating glucose uptake by peripheral tissues.

A different characterization is obtained assuming that $\tau_g = \tau_i = +\infty$, and that both kernels are expressible as the following exponentials, satisfying the constraints (2.3), (2.4):

$$\omega_g(t) = \alpha_g^2 t e^{-\alpha_g t}, \qquad \omega_i(t) = \alpha_i^2 t e^{-\alpha_i t}. \tag{4.37}$$

In this case, due to the *linear chain trick* (e.g. [8]), and adopting a change of variables $t-\theta = s$:

$$\widetilde{G}(t) = \alpha_g^2 \int_0^{+\infty} \theta G(t-\theta) e^{-\alpha_g \theta} d\theta = \alpha_g^2 \int_{-\infty}^{t} (t-s) G(s) e^{-\alpha_g (t-s)} ds, \tag{4.38a}$$

$$\widetilde{I}(t) = \alpha_i^2 \int_0^{+\infty} \theta I(t-\theta) e^{-\alpha_i \theta} d\theta = \alpha_i^2 \int_{-\infty}^{t} (t-s) I(s) e^{-\alpha_i (t-s)} ds. \tag{4.38b}$$

Denoting:

$$\begin{aligned} x_1(t) &= G(t), & x_2(t) &= I(t), \\ x_3(t) &= \int_{-\infty}^{t} (t-s) G(s) e^{-\alpha_g (t-s)} ds, & x_4(t) &= \int_{-\infty}^{t} (t-s) I(s) e^{-\alpha_i (t-s)} ds, \\ x_5(t) &= \int_{-\infty}^{t} G(s) e^{-\alpha_g (t-s)} ds, & x_6(t) &= \int_{-\infty}^{t} I(s) e^{-\alpha_i (t-s)} ds, \end{aligned} \tag{4.39}$$

the following 6-dimensional ordinary differential system is obtained:

$$\begin{cases} \dot{x}_1(t) = -K_{xg}x_1(t) - K_{xgi}\alpha_i^2 x_1(t)x_4(t) + \dfrac{T_{gh}}{V_G}, \\ \dot{x}_2(t) = -K_{xi}x_2(t) + \dfrac{T_{iGmax}}{V_I} f\big(\alpha_g^2 x_3(t)\big), \\ \dot{x}_3(t) = -\alpha_g x_3(t) + x_5(t), \\ \dot{x}_4(t) = -\alpha_i x_4(t) + x_6(t), \\ \dot{x}_5(t) = x_1(t) - \alpha_g x_5(t), \\ \dot{x}_6(t) = x_2(t) - \alpha_i x_6(t), \end{cases} \tag{4.40}$$

with the initial conditions:

$$\begin{aligned} &x_1(0) = G(0), \qquad x_3(0) = -\int_{-\infty}^{0} s e^{\alpha_g s} G(s)ds, \qquad x_5(0) = \int_{-\infty}^{0} e^{\alpha_g s} G(s)ds, \\ &x_2(0) = I(0), \qquad x_4(0) = -\int_{-\infty}^{0} s e^{\alpha_i s} I(s)ds, \qquad x_6(0) = \int_{-\infty}^{0} e^{\alpha_i s} I(s)ds. \end{aligned} \tag{4.41}$$

4.1 Local stability analysis of the discrete-delays differential system

The model considered in this subsection is the one described by (4.36). In order to study the local stability of the equilibrium point, system (4.36) is linearized around (G_b, I_b). Let $Z_G(t) = G(t) - G_b$, $Z_I(t) = I(t) - I_b$. Then:

$$\begin{cases} \dfrac{dZ_G}{dt} = -\alpha Z_G(t) - \beta Z_I(t - \tau_i), \\ \dfrac{dZ_I}{dt} = \eta Z_G(t - \tau_g) - \delta Z_I(t), \end{cases} \quad \text{with} \quad \begin{aligned} &\alpha = K_{xg} + K_{xgi} I_b, \qquad \beta = K_{xgi} G_b, \\ &\eta = \frac{T_{iGmax}}{V_I} f'(G_b), \qquad \delta = K_{xi}, \end{aligned} \tag{4.42}$$

from which the characteristic equation is:

$$d(\lambda) = \lambda^2 + (\alpha + \delta)\lambda + \alpha\delta + \beta\eta e^{-(\tau_i + \tau_g)\lambda}. \tag{4.43}$$

Note that, despite the presence of two delays in the model, the characteristic equation provides only one delay element, which is the sum of the two original delays. Moreover, by neglecting both delays ($\tau_g = \tau_i = 0$), $d(\lambda)$ reduces to a second order equation with all positive coefficients, so that its roots belong to the negative real half plane, which implies asymptotic stability of the origin of the linearized system and local asymptotic stability of the equilibrium point of the original system. The point is to see what happens by increasing one or both delays. We employ the standard imaginary root crossing method [8].

Theorem 4.8. **[8]** *Consider the following equation:*

$$\lambda^2 + a\lambda + c + de^{-\tau\lambda} = 0, \qquad a, c, d > 0, \quad \tau \geq 0. \tag{4.44}$$

If $\tau = 0$ there are only two solutions, both belonging to the negative real complex half plane. By increasing the parameter τ, pairs of conjugate complex solutions can appear in the positive real complex half plane $\mathbb{C}^+$, according to the following hypotheses:

i) $c \geq d$ *and* $2c - a^2 \leq 2\sqrt{c^2 - d^2}$*: solutions in* $\mathbb{C}^+$ *never occur;*
ii) $c < d$ *or* $\big(c = d$ *and* $2c - a^2 > 2\sqrt{c^2 - d^2}\big)$*: there exists* τ_0 *such that for* $\tau < \tau_0$ *there are no solutions in* $\mathbb{C}^+$*; for* $\tau = \tau_0$ *a pair of pure imaginary conjugate solutions occurs; for* $\tau > \tau_0$ *pairs of conjugate solutions definitively occur in* $\mathbb{C}^+$*;*
iii) $c > d$ *and* $2c - a^2 > 2\sqrt{c^2 - d^2}$*: there exist* τ_0*,* $\bar{\tau}_0$*, with* $\tau_0 < \bar{\tau}_0$*, such that for* $\tau < \tau_0$ *there are no solutions in* $\mathbb{C}^+$*; for* $\tau = \tau_0$ *a pair of pure imaginary conjugate solutions occurs; for* $\tau_0 < \tau < \bar{\tau}_0$ *pairs of conjugate solutions appear and disappear in* $\mathbb{C}^+$*, so producing a finite number of switches between presence and absence of solutions in* $\mathbb{C}^+$*; for* $\tau \geq \bar{\tau}_0$*, there will definitively be at least a pair of conjugate solutions in* $\mathbb{C}^+$*.*

Theorem 4.9. *Assume condition* (4.29) *holds true among the model parameters. Then the equilibrium point of system* (4.36) *is globally asymptotically stable, whatever the value of the delays* τ_i*,* τ_g*. Otherwise, there exists* τ_0 *such that:*
– *for* $\tau_i + \tau_g < \tau_0$ *the equilibrium point is locally asymptotically stable;*
– *for* $\tau_i + \tau_g > \tau_0$ *the equilibrium point changes definitively from stable to unstable, undergoing a supercritical Hopf bifurcation.*

Proof. Consider the linearized system (4.42) with the characteristic equation (4.43). By applying Theorem 4.8, there are no solutions in $\mathbb{C}^+$ (so ensuring local asymptotic stability of the equilibrium point) if:

$$\alpha\delta \geq \beta\eta \qquad \text{and} \qquad 2\alpha\delta - (\alpha + \delta)^2 \leq 2\sqrt{\alpha^2\delta^2 - \eta^2\beta^2}. \tag{4.45}$$

Note that, if the first condition in (4.45) holds true, then the second is also satisfied, in that:

$$2\alpha\delta - (\alpha + \delta)^2 = -(\alpha^2 + \delta^2) < 0 < \sqrt{\alpha^2\delta^2 - \eta^2\beta^2}. \tag{4.46}$$

By substituting the model parameters from (4.42) in (4.46) and explicitly taking into account the derivative $f'(G_b)$ in (2.5) and the computation of the ratio T_{iGmax}/V_I in (2.6), condition (4.29) is obtained. On the other hand, if (4.29) were not true, then condition ii) in Theorem 4.8 would be verified.

∎

Remark 4.10. Assume that $\alpha\delta < \beta\eta$. In order to determine the value of the total delay τ_0 which is the boundary between stability and instability, consider the pure imaginary roots, $r_{1/2} = \pm j\omega$, crossing the imaginary axis when $\tau_i + \tau_g$ increases, [8]:

$$-\omega^2 + j(\alpha+\delta)\omega + \alpha\delta + \beta\eta e^{-j(\tau_i+\tau_g)\omega} = 0 \quad \Rightarrow \quad \begin{cases} -\omega^2 + \alpha\delta + \beta\eta\cos\big((\tau_i + \tau_g)\omega\big) = 0, \\ (\alpha + \delta)\omega - \beta\eta\sin\big((\tau_i + \tau_g)\omega\big) = 0, \end{cases} \tag{4.47}$$

from which only one positive ω is achieved:

$$\omega = \bar{\omega} = \sqrt{\frac{-(\alpha^2 + \delta^2) + \sqrt{(\alpha^2 - \delta^2)^2 + 4\beta^2\eta^2}}{2}}. \tag{4.48}$$

According to (4.47), the pure imaginary roots occur when $\tau_i + \tau_g$ is such that:

$$\cos\big(\bar{\omega}(\tau_i + \tau_g)\big) = \frac{\bar{\omega}^2 - \alpha\delta}{\beta\eta}, \qquad \sin\big(\bar{\omega}(\tau_i + \tau_g)\big) = \frac{\bar{\omega}(\alpha + \delta)}{\beta\eta}. \tag{4.49}$$

τ_0 is the total delay $\tau_i + \tau_g$ coming from (4.49).

Remark 4.11. It is important to know whether Theorem 4.9 ensures the local stability of the model for a realistic set of parameters. Below are reported the ones estimated for a healthy subject, according to [14]:

$$\begin{array}{llll} G_b = 4.39\text{mM}, & V_G = 0.194\text{L/kgBW}, & K_{xg} = 0\text{min}^{-1}, & \tau_g = 23.50\text{min}, \\ I_b = 62.47\text{pM}, & V_I = 0.25\text{L/kgBW}, & K_{xi} = 0.059\text{min}^{-1}, & \tau_i = 0\text{min}, \\ G^* = 9\text{mM}, & \gamma = 2.52, & K_{xgi} = 5.3 \cdot 10^{-5}\text{min}^{-1}\text{pM}^{-1}, & \end{array} \tag{4.50}$$

from which:

$$T_{iGmax} = 6.547\text{min}^{-1}(\text{pmol/kgBW}), \qquad T_{gh} = 2.820 \cdot 10^{-3}\text{min}^{-1}(\text{mmol/kgBW}). \tag{4.51}$$

According to Theorem 4.9, condition (4.29) is not fulfilled, in that:

$$\frac{K_{xgi} I_b \gamma}{1 + \left(\frac{G_b}{G^*}\right)^\gamma} = 0.717 \cdot 10^{-2} > K_{xg} + K_{xgi} I_b = 0.331 \cdot 10^{-2}. \tag{4.52}$$

Nevertheless, local asymptotic stability is easily ensured because:

$$\tau_0 \simeq 308.45\text{min} \gg \tau_i + \tau_g = 23.50\text{min}. \tag{4.53}$$

4.2 Local stability analysis of the distributed delay model with exponential kernels

Taking into account the ODE representation described by (4.40), the local asymptotic stability of the equilibrium point

$$X_{\text{eq}} = \begin{pmatrix} G_b & I_b & \dfrac{G_b}{\alpha_g^2} & \dfrac{I_b}{\alpha_i^2} & \dfrac{G_b}{\alpha_g} & \dfrac{I_b}{\alpha_i} \end{pmatrix}^T \tag{4.54}$$

is achieved if and only if all the roots of the characteristic polynomial associated to the Jacobian of (4.40) computed in X_{eq}:

$$J(X_{\text{eq}}) = \begin{bmatrix} -(K_{xg} + K_{xgi} I_b) & 0 & 0 & -K_{xgi}\alpha_i^2 G_b & 0 & 0 \\ 0 & -K_{xi} & \frac{T_{iGmax}}{V_I}\alpha_g^2 f'(G_b) & 0 & 0 & 0 \\ 0 & 0 & -\alpha_g & 0 & 1 & 0 \\ 0 & 0 & 0 & -\alpha_i & 0 & 1 \\ 1 & 0 & 0 & 0 & -\alpha_g & 0 \\ 0 & 1 & 0 & 0 & 0 & -\alpha_i \end{bmatrix}, \tag{4.55}$$

have negative real part. After computations, the characteristic polynomial is:

$$d(\lambda) = \big(\lambda + (K_{xg} + K_{xgi} I_b)\big)(\lambda + K_{xi})(\lambda + \alpha_g)^2(\lambda + \alpha_i)^2 + \frac{T_{iGmax} K_{xgi} \alpha_i^2 \alpha_g^2 G_b}{V_I} f'(G_b). \tag{4.56}$$

Notice that it may be written as:

$$d(\lambda) = \prod_{i=1}^{6}(\lambda + p_i) + k, \qquad \text{with} \qquad k = \frac{T_{iGmax} K_{xgi} \alpha_i^2 \alpha_g^2 G_b}{V_I} f'(G_b), \tag{4.57}$$

and:

$$p_1 = K_{xg} + K_{xgi} I_b, \qquad p_2 = K_{xi}, \qquad p_3 = p_4 = \alpha_g, \qquad p_5 = p_6 = \alpha_i. \tag{4.58}$$

Remark 4.12. Due to (2.5) and (2.6), parameter k can be written as:

$$k = \frac{K_{xgi} K_{xi} \alpha_i^2 \alpha_g^2 I_b \gamma}{1 + \left(\frac{G_b}{G^*}\right)^{\gamma}}. \tag{4.59}$$

Typically $G_b/G^* \leq 1$, in which case, keeping fixed all parameters except γ, $k = k(\gamma)$ is a positive function diverging to $+\infty$ as γ increases, with $k(0) = 0$. If it were $G_b/G^* > 1$, keeping fixed all the parameters except γ, $k = k(\gamma)$ would be a positive bounded function for $\gamma \geq 0$, admitting a single maximum for γ satisfying the following equation:

$$\left(\frac{G_b}{G^\star}\right)^{\gamma} - \gamma \left(\frac{G_b}{G^\star}\right)^{\gamma} \log\left(\frac{G_b}{G^\star}\right) + 1 = 0. \tag{4.60}$$

From (4.59), it is apparent that k strongly depends on the parameters p_i. Nevertheless, due to Remark 4.12, $k = k(\gamma)$ may well be unbounded w.r.t. γ, so that we can assume without loss of generality $k \in [0, +\infty)$. If it were $k = 0$, it would easily follow that $d(\lambda)$ has 6 negative real roots, so that the equilibrium point would be locally asymptotically stable. The point is to see whether the stability changes by increasing $k > 0$. The analysis is based on well known results of feedback control law design, such as the *root locus method* [3] and *Routh-Hurwitz criterion* [15]. More details can be found in [4, 5].

Theorem 4.13. *Consider system* (4.40). *There exists a critical value* $\bar{k} \in \mathbb{R}^+$ *such that the equilibrium point* (4.54) *is locally asymptotically stable if and only if the following condition is satisfied:*

$$\frac{K_{xgi} K_{xi} \alpha_i^2 \alpha_g^2 I_b \gamma}{1 + \left(\frac{G_b}{G^*}\right)^{\gamma}} < \bar{k}. \tag{4.61}$$

Otherwise, the equilibrium point is unstable.

Proof. As previously written, the equilibrium point is asymptotically stable if, and only if, the roots of the characteristic equation (4.57) all belong to the negative real complex half plane. Note that the roots of the characteristic polynomial $d(\lambda)$ are exactly the closed loop poles of the feedback control system described in fig. 4.1, when a unitary feedback is performed, with the SISO (Single-Input/Single-Output) open loop transfer function given by $W(\lambda)$ (see [4]).

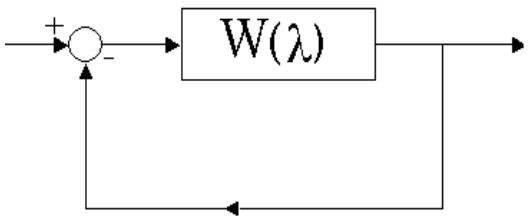

$$W(\lambda) = \frac{k}{\prod_{i=1}^{6}(\lambda + p_i)}.$$

Fig. 4.1. Closed loop control scheme.

The plots on the complex plane described by the six roots of $d(\lambda)$ when k positively increases from 0 to $+\infty$ consist of the positive root locus of $W(\lambda)$ [4]. When $k = 0$, the root locus consists of 6 negative real points, coinciding with the roots $-p_i$. There are no zeros for $W(\lambda)$, so that, by making $k > 0$ increase, each locus asymptotically follows one of 6 half lines, all of them crossing the center C situated on the real axis at the x-coordinate given by:

$$C = -\frac{\sum_{i=1}^{6} p_i}{6}. \tag{4.62}$$

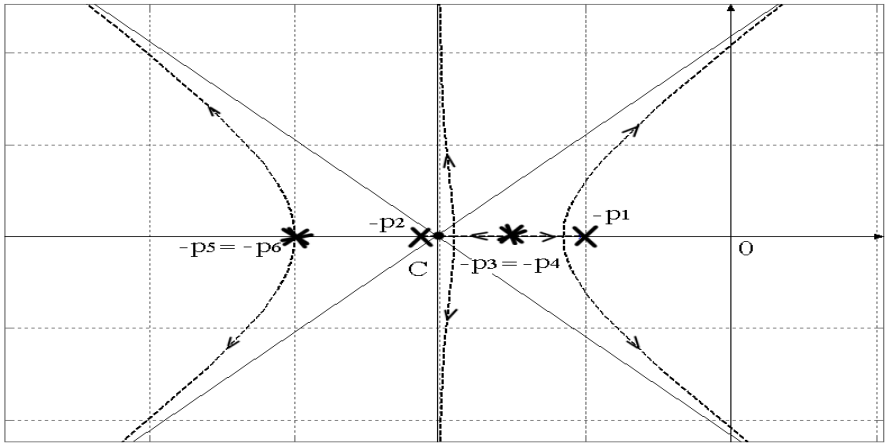

Fig. 4.2. Root locus.

The 6 half lines cross the real axis with the angles: $(\pi + 2h\pi)/6$, $h = 0, 1, \ldots, 5$. Figure 4.2 qualitatively describes the root locus in the complex plane for a set of parameters such that: $-p_5 = -p_6 < -p_2 < C < -p_3 = -p_4 < -p_1 < 0$. Each locus starts at $k = 0$ from the crosses in the picture; the grey lines are the asymptotes, each passing through the center C (a bold circle in the picture). Figure 4.3 zooms on the two loci crossing the imaginary axis. Looking at the qualitative behavior of the 6 root loci, we see that two of them cross the imaginary axis (symmetrically w.r.t. the origin), which means that there exists a positive $\bar{k}$ such that:

- for $k < \bar{k}$ all the roots are in the negative real complex half-plane;
- for $k = \bar{k}$ there is a pair of conjugate pure imaginary complex roots; all the other are in the negative real complex half-plane;
- for $k > \bar{k}$ there is a pair of conjugate complex roots in the positive real complex half-plane.

Local asymptotic stability is then ensured for $k < \bar{k}$.

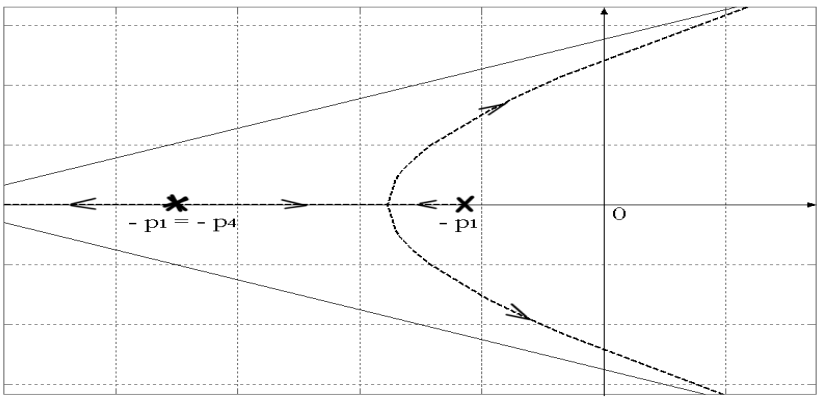

Fig. 4.3. Zoom of the root loci crossing the imaginary axis.

The computation of $\bar{k}$ is left to the Routh-Hurwitz criterion, which is reported below for the ease of the reader.

Theorem 4.14. **[15]** *Consider the polynomial equation:*

$$p(\lambda) = \alpha_n \lambda^n + \alpha_{n-1}\lambda^{n-1} + \cdots + \alpha_1 \lambda + \alpha_0 = 0, \qquad \alpha_n > 0, \tag{4.63}$$

and compute the following table:

n	a_n^0	a_{n-2}^0	a_{n-4}^0	a_{n-6}^0	$\cdots$
$n-1$	a_{n-1}^1	a_{n-3}^1	a_{n-5}^1	a_{n-7}^1	$\cdots$
$n-2$	a_{n-2}^2	a_{n-4}^2	a_{n-6}^2	$\cdots$	
$\vdots$	$\vdots$	$\vdots$			
2	a_2^{n-2}	a_0^{n-2}			
1	a_1^{n-1}				
0	a_0^n				

Table 4.1. Routh-Hurwitz table

according to the rules:

i) $a_i^0 = \alpha_i, \qquad i = n, n-2, n-4, \ldots;$

ii) $a_i^1 = \alpha_i, \qquad i = n-1, n-3, n-5, \ldots;$

iii) $a_i^j = -\dfrac{b_i^j}{a_{n+1-j}^{j-1}}, \quad b_i^j = \begin{vmatrix} a_{n+2-j}^{j-2} & a_i^{j-2} \\ a_{n+1-j}^{j-1} & a_{i-1}^{j-1} \end{vmatrix}, \quad j = 2, 3, \ldots, n, \quad i = n-j, n-j-2, \cdots.$

Then, the roots of (4.63) *have all negative real part if and only if the coefficients of the first column of the table (i.e.* $a_n^0, a_{n-1}^1, \ldots, a_0^n$*) are all positive.*

∎

The Routh-Hurwitz table is computed for the following polynomial:

$$d(\lambda) = \lambda^6 + a_5\lambda^5 + a_4\lambda^4 + a_3\lambda^3 + a_2\lambda^2 + a_1\lambda + a_0 + k, \qquad a_i > 0, \tag{4.64}$$

derived by expanding the products in (4.57) with:

$$\begin{aligned} a_5 &= \sum_{i=1}^{6} p_i, & a_4 &= \sum_{i_j \neq i_k} p_{i_j} p_{i_k}, & a_3 &= \sum_{i_j \neq i_k} p_{i_1} p_{i_2} p_{i_3}, \\ a_2 &= \sum_{i_j \neq i_k} p_{i_1} p_{i_2} p_{i_3} p_{i_4}, & a_1 &= \sum_{i_j \neq i_k} p_{i_1} p_{i_2} p_{i_3} p_{i_4} p_{i_5}, & a_0 &= p_1 p_2 p_3 p_4 p_5 p_6. \end{aligned} \tag{4.65}$$

6	1	a_4	a_2	a_0+k
5	a_5	a_3	a_1	
4	b_1	b_2	a_0+k	
3	c_1	$c_2(k)$		
2	$d_1(k)$	a_0+k		
1	$e_1(k)$			
0	a_0+k			

$$b_1 = \frac{a_4a_5 - a_3}{a_5}, \qquad b_2 = \frac{a_2a_5 - a_1}{a_5},$$
$$c_1 = \frac{a_3b_1 - a_5b_2}{b_1}, \quad c_2(k) = \frac{a_1b_1 - a_5(a_0+k)}{b_1},$$
$$d_1(k) = \frac{b_2c_1 - b_1c_2(k)}{c_1},$$
$$e_1(k) = \frac{c_2(k)d_1(k) - c_1(a_0+k)}{d_1(k)}.$$

Table 4.2. Routh-Hurwitz table of the characteristic polynomial (4.57).

Recall that for $k = 0$ all roots are real negative, so that $b_1 > 0$, $c_1 > 0$ and:

$$\begin{aligned} d_1(0) > 0 \qquad &\Longrightarrow \qquad b_2c_1 - a_1b_1 + a_0a_5 > 0, \\ e_1(0) > 0 \qquad &\Longrightarrow \qquad c_2(0)\big(b_2c_1 - b_1c_2(0)\big) - a_0c_1^2 > 0. \end{aligned} \tag{4.66}$$

According to the Routh-Hurwitz criterion, we must find when $d_1(k) > 0$ and $e_1(k) > 0$. Note that:

$$d_1(k) = d_1(0) + \frac{a_5k}{c_1} > 0, \qquad \forall k > 0, \tag{4.67}$$

so that only the condition $e_1(k) > 0$ (or equivalently $e_1(k)d_1(k) > 0$) has to be checked, with:

$$\begin{aligned} e_1(k)d_1(k) &= \left(c_2(0) - \frac{a_5k}{b_1}\right)\left(d_1(0) + \frac{a_5k}{c_1}\right) - c_1a_0 - c_1k \\ &= -\frac{a_5^2}{b_1c_1}k^2 + \left(\frac{a_5c_2(0)}{c_1} - \frac{a_5d_1(0)}{b_1} - c_1\right)k + e_1(0)d_1(0). \end{aligned} \tag{4.68}$$

Notice that $e_1(k)d_1(k)$ is a second order polynomial (w.r.t. k) of the type:

$$\alpha k^2 + \beta k + \eta, \qquad \text{with} \qquad \alpha < 0, \quad \eta > 0, \tag{4.69}$$

so that it always admits a pair of real roots (one positive, the other negative). The critical value $\bar{k}$ is the positive root of (4.69), given by:

$$\bar{k} = \frac{b_1c_1}{2a_5^2}\left(\frac{a_5c_2(0)}{c_1} - \frac{a_5d_1(0)}{b_1} - c_1 + \sqrt{\left(\frac{a_5c_2(0)}{c_1} - \frac{a_5d_1(0)}{b_1} - c_1\right)^2 + \frac{4e_1(0)d_1(0)a_5^2}{b_1c_1}}\right). \tag{4.70}$$

Remark 4.15. In this case also it is important to see whether Theorem 4.13 ensures the local stability of the model for a realistic set of parameters, as the ones that follow:

$$\begin{aligned} &G_b = 4.39\text{mM}, \qquad &&V_G = 0.259\text{L/kgBW}, \qquad &&K_{xg} = 0\text{min}^{-1}, \qquad &&\alpha_g = 0.106\text{min}^{-1}, \\ &I_b = 62.50\text{pM}, \qquad &&V_I = 0.136\text{L/kgBW}, \qquad &&K_{xi} = 0.113\text{min}^{-1}, \qquad &&\alpha_i = 0.123\text{min}^{-1}, \\ &G^* = 9\text{mM}, \qquad &&\gamma = 2.66, \qquad &&K_{xgi} = 4.43 \cdot 10^{-5}\text{min}^{-1}\text{pM}^{-1}, \end{aligned} \tag{4.71}$$

from which:

$$T_{iGmax} = 7.444\text{min}^{-1}(\text{pmol/kgBW}), \qquad T_{gh} = 3.148 \cdot 10^{-3}\text{min}^{-1}(\text{mmol/kgBW}). \tag{4.72}$$

According to the Routh-Hurwitz criterion:

$$\frac{K_{xgi}K_{xi}\alpha_i^2\alpha_g^2 I_b\gamma}{1+\left(\frac{G_b}{G^*}\right)^{\gamma}} = 1.232 \cdot 10^{-7} < \bar{k} = 9.835 \cdot 10^{-7}. \tag{4.73}$$

5. Simulation results

In order to gain insight on the likely behavior of the solutions, two kind of simulation studies were performed.

In the first study, we explored violations to the criterion for local stability. We took the total delay $\tau_i + \tau_g$ very large for the discrete delay model, or γ very large for the distributed delay model. We started trajectories in a relatively small neighborhood of the equilibrium solution $\big(G(0) \in (3\text{mM}, 7\text{mM}), I(0) \in (40\text{pM}, 80\text{pM})\big)$. In these cases we observed actual limit cycles established as $t \mapsto +\infty$. In figure 5.1 three limit cycles are reported for the discrete-delay model according to three different values of τ_g; all the other parameter values are taken from Remark 4.11. According to the critical value $\tau_0 \simeq 308.45$ min, τ_g has been chosen equal to 310 min, 400 min, 500 min.

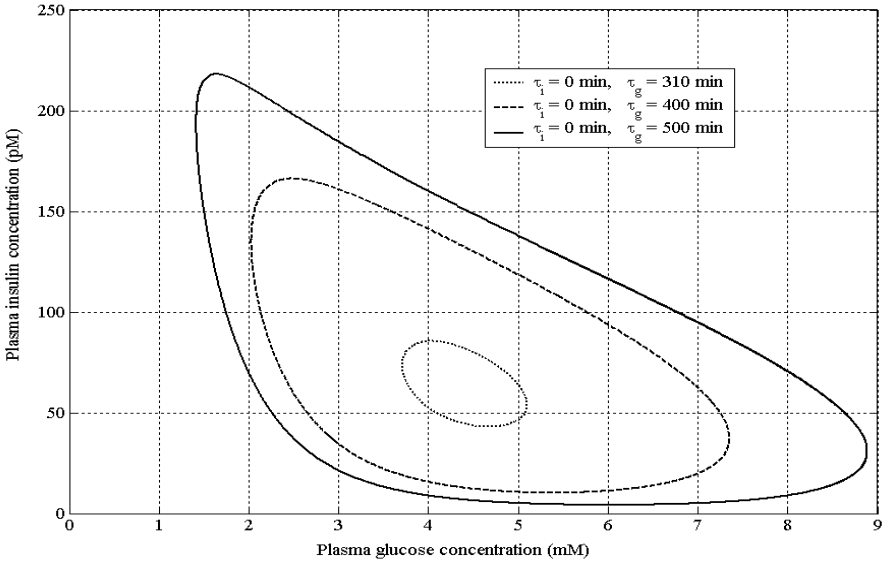

Fig. 5.1. Limit cycles of the discrete-delay model.

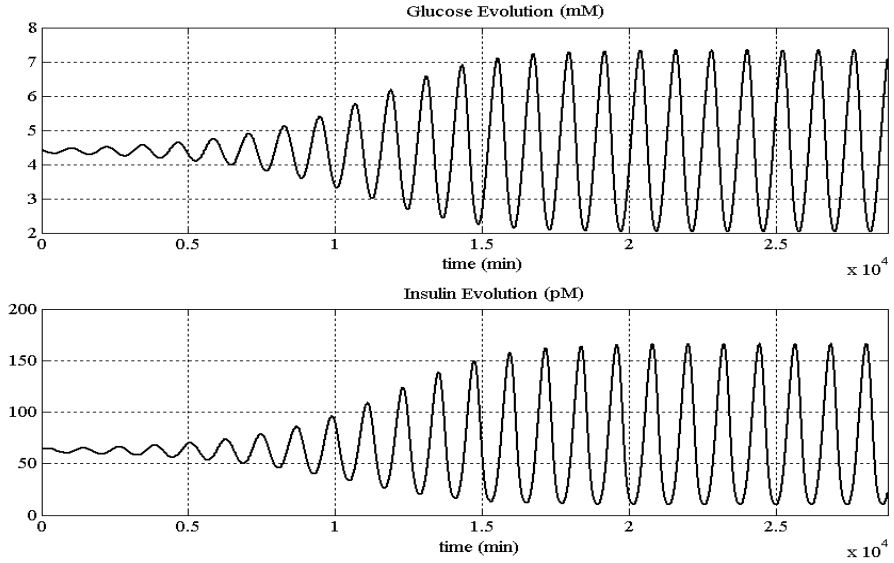

Fig. 5.2. Glucose/insulin evolution for the discrete-delay model with $\tau_g = 400$ min.

In figure 5.2 the glucose/insulin time response, over a range of 20 days is reported for the case of $\tau_g = 400$ min. The initial conditions are the ones of an IVGTT (3.2), with $D_g = 0.01$mmol/kgBW and $I_\Delta = 56.97$pM/mM. As a matter of fact, both $G_\Delta = 0.0515$mM and $I_\Delta G_\Delta = 2.9366$pM are very small perturbations of the equilibrium point $(G_b, I_b) = (4.39\text{mM}, 62.47\text{pM})$. Nevertheless, figure 5.3 shows clearly the limit cycle occurring because the total delay $\tau_g + \tau_i = 400$ min is greater than the critical value $\tau_0 \simeq 308.45$ min.

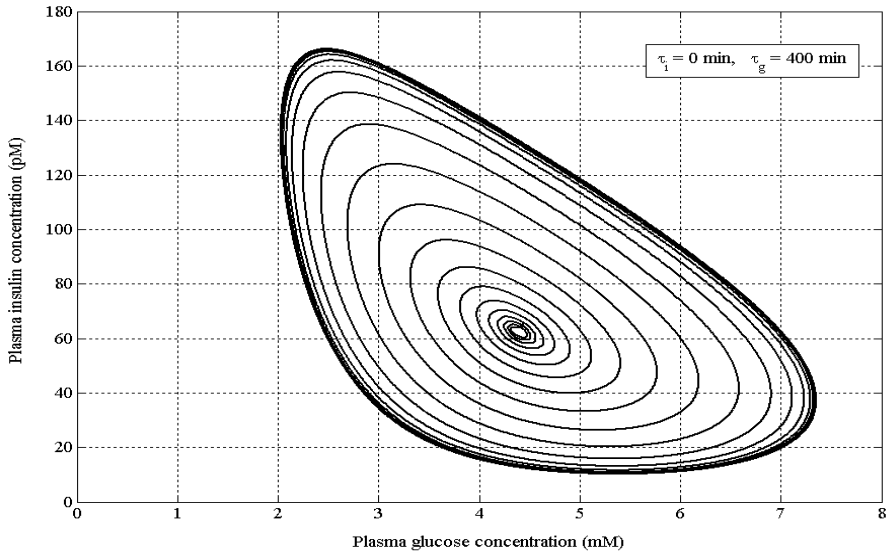

Fig. 5.3. Occurring of the limit cycle for the discrete-delay model with $\tau_g = 400$ min.

Remark 4.16. While the behavior of the system as the delay is increased beyond the critical value is of mathematical interest, it should be kept in mind that the situation depicted is far from physiological: not only the total delay is about twenty times that observed in a healthy volunteer, but the simulation rolls on for twenty days assuming the absence of further perturbations, like meals.

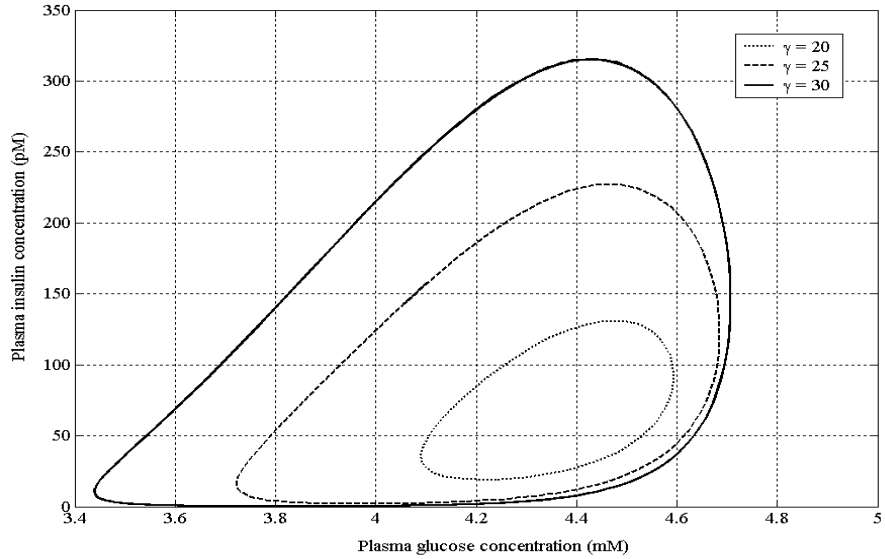

Fig. 5.4. Limit cycles of the distributed-delay model.

The same reasoning has been followed to deal with the limit cycles of the distributed delay model. In figure 5.4 three limit cycles are reported for the distributed-delay model according to three different values of γ; all the other parameter values are taken from Remark 4.15. According to the critical value $\bar{k} \simeq 9.835 \cdot 10^{-7}$, γ has been chosen equal to 20, 25, 30 (it is easy to verify that condition (4.61) is not fulfilled for these three cases). In figure 5.5 the glucose/insulin time response, over a range of 3 days is reported for the case of $\gamma = 20$. The initial conditions are the ones of an IVGTT (3.2), with $D_g = 0.01$mmol/KgBW and $I_\Delta = 111$pM/mM. Both $G_\Delta = 0.0386$Mm and $I_\Delta G_\Delta = 4.2857$pM are very small perturbations of the equilibrium point $(G_b, I_b) = (4.39\text{mM}, 62.50\text{pM})$. Nevertheless, figure 5.6 shows clearly the limit cycle occurring because condition (4.61) is violated. For the distributed-delay model also, the situation depicted is far from physiological, as stressed in Remark 4.16.

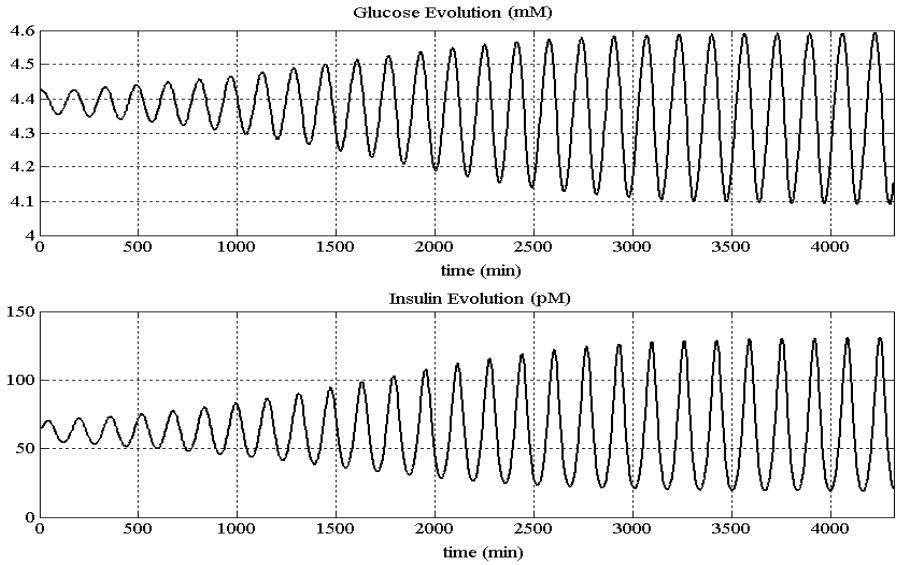

Fig. 5.5. Glucose/insulin evolution for the distributed-delay model with $\gamma = 20$.

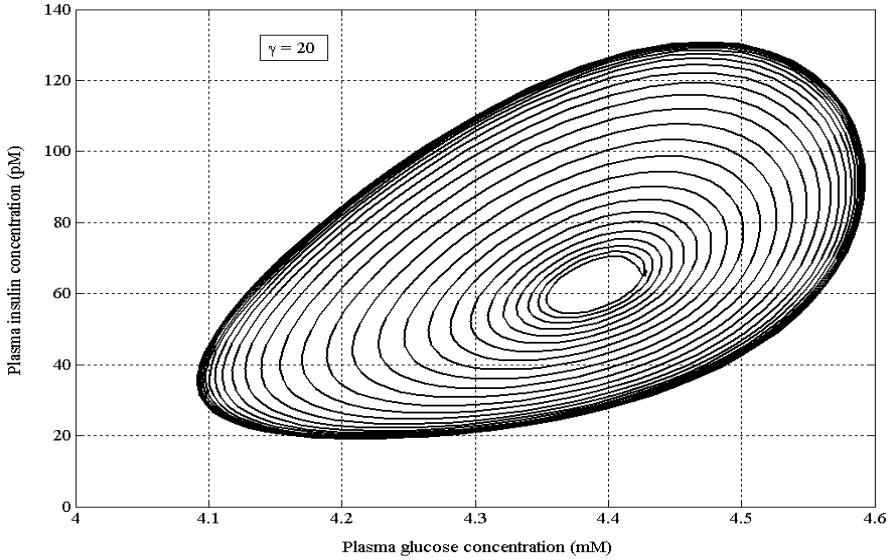

Fig. 5.6. Occurrence of the limit cycle for the distributed-delay model with $\gamma = 20$.

The second class of simulations investigates the convergence to the equilibrium point X_e (assuming conditions for local stability fulfilled for both the models), when the initial state is far from X_e. As far as the discrete-delay model is concerned, all parameter values are taken from Remark 4.11 (parameter τ_g included). The initial conditions are the ones of an IVGTT, with $I_\Delta = 56.97$pM/mM. Three simulations have been reported, over a range of 3 hours, according to three different values for the injected glucose bolus D_g, equal to 1.833 mmol/kgBW, 5 mmol/kgBW, 10 mmol/kgBW. Note that these choices produce at time zero a very large increase of both glucose and insulin concentrations, as reported in fig. 5.7, which means that the system evolution starts from an initial state far from the equilibrium. Nevertheless, the equilibrium point is reached in about two hours from the beginning of the simulations.

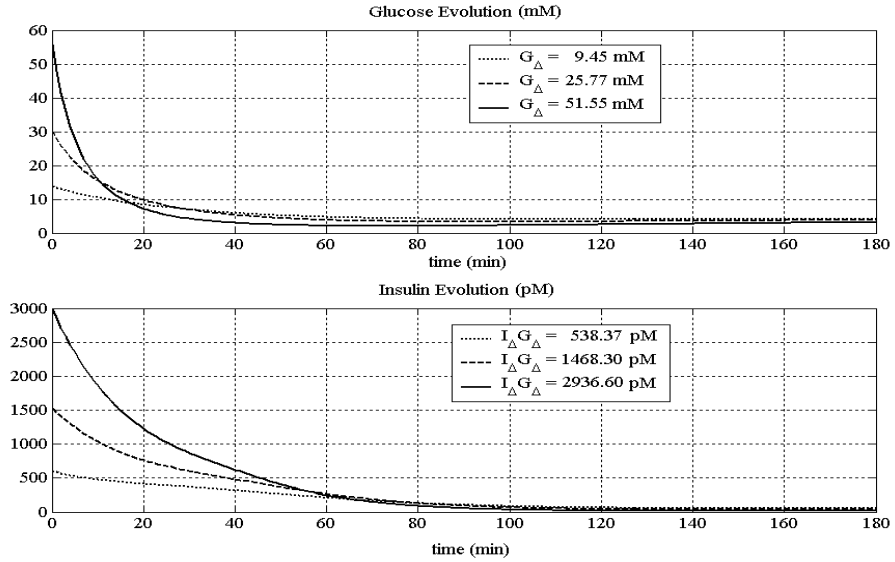

Fig. 5.7. Glucose/insulin evolution for the discrete-delay model with $\tau_g = 23.50$ min.

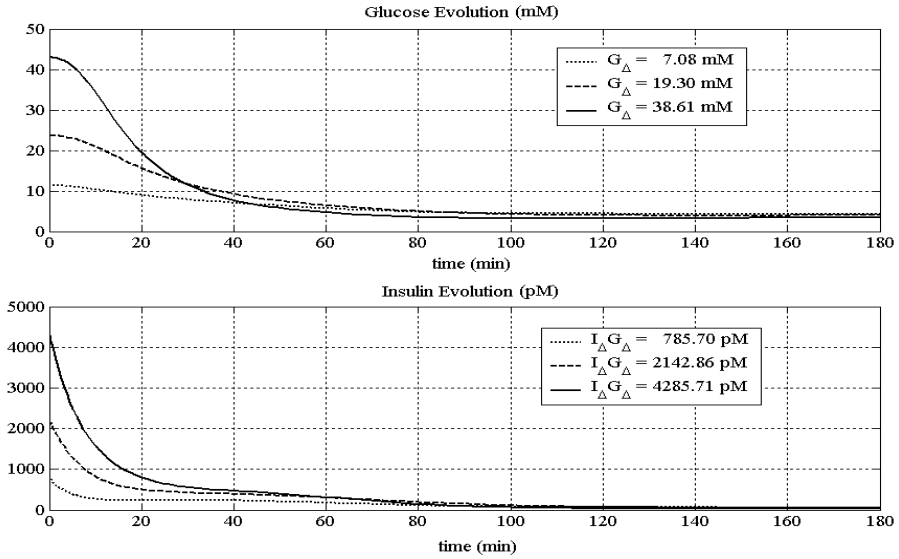

Fig. 5.8. Glucose/insulin evolution for the distributed-delay model with $\gamma = 2.66$.

As far as the distributed-delay model is concerned, all parameter values are taken from Remark 4.15 (parameter γ included). The initial conditions are the ones of an IVGTT, with $I_\Delta = 111$pM/mM. Three simulations have been reported, over a range of 3 hours, according to three different values for the injected glucose bolus D_g, equal to 1.833 mmol/kgBW, 5 mmol/kgBW, 10 mmol/kgBW (also in this case, the choices of D_g produce at time zero a very large increase of both glucose and insulin concentrations, as reported in fig. 5.8). The glucose/insulin evolutions are reported in fig. 5.8.

6. Numerical integration and estimation

The model may be identified from IVGTT data in a standard way (WLS, GLS), where the solution is computed numerically starting from initial conditions determined by the intra-venous instantaneous injection of a glucose bolus D_g, (3.2). The administered dose of glucose D_g is fixed by the investigator, while I_Δ is a further parameter to be identified. By construction, and respecting the physical properties of the experiment, all system parameters are positive. Figure 6.1 gives an example, for one subject, of the ability of the discrete- and distributed-delay models to fit experimental data.

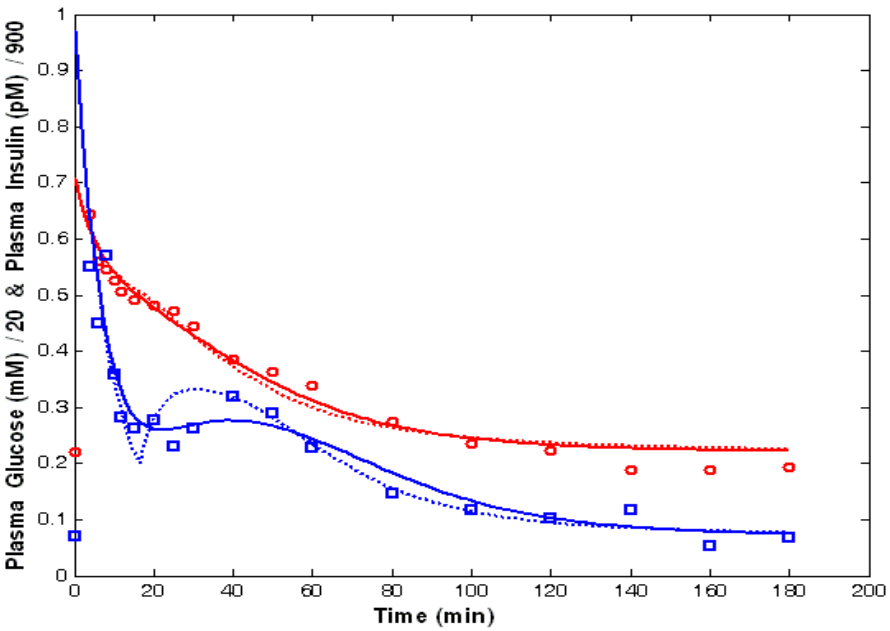

Fig. 6.1. Observed and predicted values for the glucose-insulin system.

The figure shows the insulin (squares) and glucose (circles) observed concentrations versus time, together with the predicted time-curves from the discrete-delay (dotted lines) and the distributed-delay models (solid lines). The most evident difference between the two models is, as expected, the discontinuity in the derivative which is observable in the discrete model at a time corresponding with the delayed impulsive insulin release: this produces a sharp upward corner which is absent in the corresponding distributed-delay insulin forecast. For this subject, similarly with what is observed in several others, the secondary insulin release profile as predicted by the discrete-delay model is more pronounced with respect to what is predicted by the distributed-delay model for the same observations: this does not translate necessarily in a

better fit, though, since R^2 and Akaike criterion values are generally similar for the two models on the same data. See [14] for more details.

7. Conclusions

A family of delay differential models, and more particularly two of its members (one with discrete delays and one with distributed delays) have been investigated in this work, determining several qualitative properties of the solutions. Theorems have been presented, which show existence and uniqueness of positive bounded solutions and persistence of the entire family. As far as the stability properties are concerned, conditions on the parameters are given in order to check local asymptotic stability and global stability. While conditions for local stability are easily verified over a wide range of realistic parameters values, the conditions on global stability which we could find are not verified for physiologically plausible parameter values, contrary to empirical results from simulations, showing convergence to the equilibrium solution over a very wide range of initial conditions. Given the practical usefulness of these models, more analytical work is indicated in the direction of proving analytically the stable global dynamics conjectured from simulations.

Acknowledgment.

This paper is dedicated to the memory of Ovide Arino, who inspired many of the solutions adopted here and whose lasting human and scientific influence is acutely felt by his disciples.

References

[1] R. N. Bergman, Y. Z. Ider, C. R. Bowden and C. Cobelli, "Quantitative estimation of Insulin sensitivity," *Am. Journal on Physiology,* Vol. 236, pp. 667–677, 1979.

[2] A. De Gaetano, O. Arino, "Mathematical modelling of the intravenous glucose tolerance test," *Journal of Mathematical Biology,* Vol. 40, No. 2, pp. 136–168, 2000.

[3] W. R. Evans, "Graphical analysis of control systems," *Amer. Institute Electrical Engineers (AIEE) Trans. Part II,* Vol. 67, pp. 547–551, 1948.

[4] G. F. Franklin, J. D. Powell, A. E. Naeini, *Feedback control for dynamic systems*, Addison-Wesley, 1993.

[5] F. R. Gantmacher, *The theory of matrices*, New York, Chelsea Publishing Company, 1959.

[6] J. K. Hale, S. M. Verduyn Lunel, *Introduction to functional differential equations*, Springer Verlag, New York, 1993.

[7] V. Kolmanovskii, A. Myshkis, *Introduction to the theory and applications of functional differential equations*, Kluwer Academic Publishers, Dordrecht, The Netherlands, 1999.

[8] Y. Kuang, *Delay Differential Equations with Applications in Population Dynamics*, Vol. 191, in the series of Mathematics in Science and Engineering, Academic Press, Boston, 1993.

[10] Y. Lenbury, D. V. Giang, "Nonlinear delay differential equations involving population growth," *Mathematical and Computer Modelling,* Vol. 40, pp. 583–590, 2004.

[11] J. Li, Y. Kuang, B. Li, "Analysis of IVGTT glucose-insulin interaction models with time-delay," *Discrete and Continuous Dynamical Systems-Series B,* Vol. 1, No. 1, pp. 103–124, 2001.

[12] A. Makroglou, J. Li, Y. Kuang, "Mathematical models and software tools for the glucose-insulin regulatory system and diabetes: an overview," *to appear on Applied Numerical Mathematics.*

[13] A. Mukhopadhyay, A. De Gaetano, O. Arino, "Modelling the intra-venous glucose tolerance test: a global study for a single distributed delay model," *Discrete and Continuous Dynamical Systems-Series B,* Vol. 4, No. 2, pp. 407–417, 2004.

[14] S. Panunzi, P. Palumbo and A. De Gaetano, "Modeling IVGTT data with delay differential equations," *IASI-CNR Research Report*, No.625, 2004.

[15] R. J. Routh, "A treatise on the stability of a given state of motion," Adams Prize Essay, Univ. Cambridge, England, 1877.

[16] S. H. Saperstone, *Semidynamical systems in infinite dimensional spaces*, New York: Springer Verlag, 1981.

[17] G. Toffolo, R. N. Bergman, D. T. Finegood, C. R. Bowden, C. Cobelli, "Quantitative estimation of beta cell sensitivity to glucose in the intact organism: a minimal model of insulin kinetics in the dog," *Diabetes,* Vol. 29, pp. 979–990, 1980.